Published in Vadose Zone Journal 3, issue 4, 1276-1285, 2004
which should be used for any reference to this work

Radon-222 as a Tracer for Nonaqueous Phase Liquid in the Vadose Zone: Experiments and Analytical Model

Patrick Höhener* and Heinz Surbeck

ABSTRACT

The potential use of the naturally occurring noble gas ^{222}Rn as a tracer for vadose zone contamination by nonaqueous phase liquids (NAPLs) is studied experimentally and theoretically. *n*-Dodecane was chosen as the model NAPL. In batch experiments containing unsaturated alluvial sand, a 2.9-fold decrease of the steady-state ^{222}Rn activity in soil gas was measured as a consequence of the increase in the volumetric NAPL content from 0 to 0.074. A one-dimensional analytical reactive transport model was developed that includes ^{222}Rn production, gas-phase diffusion, partitioning, and radioactive decay. Radon-222 soil gas profiles were predicted for homogeneous and heterogeneous sandy profiles where NAPL contamination was restricted to selected depth layers. The resulting depth profiles document that the position of the NAPL has great influence on the ^{222}Rn activity depth profile. An outdoor lysimeter experiment was performed using unsaturated alluvial sand contaminated by NAPL at depths from 1 to 1.2 m. In the lysimeter experiment, a spill of 2 L m^{-2} NAPL did not alter significantly the ^{222}Rn profile, as predicted also by model calculations. We concluded that ^{222}Rn can be used as a NAPL tracer in the vadose zone only at heavily polluted sites with uniform spatial ^{222}Rn production.

Spills of NAPLs, such as petroleum products or solvents, to the subsurface are a major problem at many industrial or military sites (Boulding, 1996). Knowledge of the spatial distribution and quantity of NAPL in the subsurface is crucial for optimal management and remediation of polluted sites. During the migration of NAPLs through the vadose zone, a certain amount of liquid is retained in the pores of the vadose zone by capillary forces. This fraction is known as residual saturation and may occupy up to 20% of the available pore space (Mercer and Cohen, 1990). The presence of NAPLs defines the so-called source zone (Wiedemeier et al., 1999), from which gaseous and aqueous contaminant plumes are formed. Source zone delineation is a key procedure at any NAPL-contaminated site. Delineation of source zones with traditional sampling techniques (e.g., soil cores, trenches) presents considerable difficulties and costs (Feenstra and Cherry, 1996). Soil gas monitoring is often used as an exploratory method at sites where the vadose zone has been contaminated with NAPL containing volatile organic compounds (VOCs, Wilson, 1997; Looney and Falta, 2000). High VOC concentrations are associated with the source zones (Werner et al., 2004). Measured vapor concentration profiles can be used to approximately locate these source zones and for describing lateral or vertical extensions of contaminant vapor plumes emanating from them (Robbins et al., 1990; Wilson, 1997; Pasteris et al., 2002). However, the contaminant vapor concentrations in the subsurface are by themselves not an indication of the amount of NAPL residual in the source zone. A method for NAPL quantification based on the measurement of a gaseous compound would therefore be a useful complement to traditional vadose zone soil gas monitoring. For the vadose zone, the use of gaseous tracers is especially promising because their use can be combined easily with conventional soil gas monitoring (Werner et al., 2004). Artificial gaseous partitioning tracers have been introduced in recent years for NAPL quantification in the vadose zone (Deeds et al., 1999; Mariner et al., 1999; Whitley et al., 1999; Werner, 2002; Werner and Höhener, 2002a; Brusseau et al., 2003). The tracers may be transported by advection (Mariner et al., 1999) or diffusion (Werner and Höhener, 2002a) through the soil volume of interest. Interpretation of tracer breakthrough curves yields the average volumetric NAPL content of the vadose zone (Dwarakanath et al., 1999). However, the injection of artificial tracers into the vadose zone and the analysis of breakthrough curves requires technical equipment and ample time on the site and hence may be costly.

A more simple way of making use of a gaseous tracer is to take advantage of a native soil gas that partitions into NAPLs. The naturally occurring isotope ^{222}Rn of the noble gas Rn is such a gas and has been proposed previously as a partitioning tracer for NAPL contamination in both the vadose zone (Meissner et al., 2000; Schubert et al., 2000, 2001, 2002; Schubert, 2001) and the saturated zone (Hunkeler et al., 1997; Semprini et al., 2000; Davis et al., 2002). Radon-222 is produced by α-particle decay of ^{226}Ra, an isotope of the natural radioactive decay series of ^{238}U (Cecil and Green, 1999). Radon-222 itself decays by α-particle decay, with a half-life of 3.8 d to a series of short-lived daughter products (^{218}Po, ^{214}Pb, ^{214}Bi, ^{214}Po; Nazaroff, 1992; Van der Spoel et al., 1997). From minerals that contain ^{226}Ra, ^{222}Rn emanates to the surrounding gas or water phase by α recoil and diffusion (Hoehn and von Gunten, 1989; Nazaroff, 1992). Radon-222 is a chemically inert noble gas; however, it partitions into NAPL (Hunkeler et al., 1997). When groundwater containing ^{222}Rn at emanation–decay steady-state activity migrates into a NAPL-contaminated zone of an aquifer, the ^{222}Rn activity in the water phase decreases due to partitioning of ^{222}Rn between the NAPL and the water (Hunkeler et al., 1997). In vadose zone NAPL source zones with uniform ^{226}Ra

P. Höhener, Swiss Federal Institute of Technology (EPFL), ENAC-ISTE-LPE, CH-1015 Lausanne, Switzerland; H. Surbeck, University of Neuchâtel, Center for Hydrogeology (CHYN), Rue Emile Argand 11, CH-2007 Neuchâtel, Switzerland. Received 20 Nov. 2003. Original Research Paper. *Corresponding author: (patrick.hoehener@epfl.ch).

Abbreviations: NAPL, nonaqueous phase liquid; TDR, time domain reflectometry; VOC, volatile organic compound.

distributions, ^{222}Rn activities measured in the soil gas may decrease similarly. Schubert and coworkers presented experimental evidence for local ^{222}Rn minima in NAPL source zones in a lysimeter (Schubert et al., 2000) and for two field cases at abandoned gasoline stations (Schubert et al., 2001). They suggested that, as a general rule, ^{222}Rn activities decrease at every NAPL-contaminated site compared with profiles at uncontaminated sites nearby. They stated also that ^{222}Rn activity profiles in the vadose zone vary as a function of depth, boundary conditions at depth, and vadose zone water content. However, a detailed study of ^{222}Rn profiles in heterogeneously contaminated vadose zones including modeling of pertinent transport and partitioning processes, is lacking. Contrary to the work by Schubert et al., it is likely that the ^{222}Rn activities may either increase or decrease at certain locations in heterogeneously contaminated profiles compared with a reference profile, depending on the position of the NAPL layer in the subsurface. A NAPL layer residing near the soil surface could hinder ^{222}Rn transport to the atmosphere. It has been shown that sealing of the soil surface (e.g., by a road) leads to increased ^{222}Rn activities in the vadose zone (Wiegand, 2001).

The aim of this paper is (i) to present a general model for ^{222}Rn transport in homogeneous and heterogeneous NAPL-contaminated vadose zones; (ii) to verify basic relevant assumptions of the model experimentally by means of batch experiments; (iii) to model the ^{222}Rn activities in the vadose zone as a function of depth, volumetric water or NAPL content, and NAPL location; and (iv) to compare a selected model realization with profiles measured in a lysimeter with a low NAPL contamination.

THEORY AND ANALYTICAL MODEL

Relevant Assumptions

The theory presented here relies on the following assumptions: The vadose zone is described as a homogeneous porous medium with uniform and constant properties. In particular, we assume that ^{226}Ra activity is constant in space and time, and hence that ^{222}Rn is produced uniformly throughout the vadose zone. The phases of the porous medium are soil air, soil water, NAPL, and the solid matrix. Partitioning of ^{222}Rn between the phases is described by instantaneous, reversible linear equilibrium. Gas-phase diffusion is the only relevant transport process, and radioactive decay is the only reaction. Soil air, soil water, and NAPL are further assumed to be immobile, and steady state is assumed for diffusive gas transport and Ra–Rd decay. Both fluids, NAPL and water, influence the effective gas-phase diffusion coefficient; the model of Millington and Quirk (1961) is used to account for these effects.

Partitioning of ^{222}Rn in an NAPL-Contaminated Vadose Zone

Assuming instantaneous linear equilibrium between the air, water, NAPL, and solid phases, the partitioning of ^{222}Rn can be described using the air–water partitioning coefficient (Henry coefficient) H, the solid–water partitioning coefficient K_d, and the air–NAPL partitioning coefficient K_n (for notations and units see Table 1). The fraction f_i of ^{222}Rn in the air phase of layer i can be calculated using (Werner and Höhener, 2002a)

$$f_i = \frac{1}{1 + \dfrac{\rho_s(1 - \theta_t)K_d}{H\theta_a} + \dfrac{\theta_w}{H\theta_a} + \dfrac{\theta_n}{K_n\theta_a}} \quad [1]$$

where θ_a, θ_w, θ_n, and θ_t denote air-filled, water-filled, NAPL-filled, and total porosities, respectively, and ρ_s denotes the density of the solids. Note that the inverse value of f_i is equal to the retardation coefficient $R = f_i^{-1}$, a quantity used for the interpretation of advective partitioning tracer tests (Brusseau et al., 2003).

General Equation for ^{222}Rn Diffusion in the Vadose Zone

If decay is described by a single first-order rate constant λ, the governing equation for one-dimensional diffusion-dominated transport in a porous medium with uniform and constant properties can be written as

$$\frac{\partial A}{\partial t} = f_i D_i \frac{\partial^2 A}{\partial z^2} - \lambda A + f_i S_i \quad [2a]$$

where A is the activity of ^{222}Rn in soil air (kBq m^{-3}) and D_i is the effective gas-phase diffusion coefficient of ^{222}Rn in soil air of layer i, defined as

$$D_i = \tau D_m \quad [2b]$$

where D_m is the molecular diffusion coefficient of ^{222}Rn in air. The tortuosity factor τ is described using the model of Millington and Quirk (1961):

$$\tau = \theta_a^{2.33}/\theta_t^2 \quad [2c]$$

The production rate of ^{222}Rn in pore space S_i is related to the Ra concentration according to (Van der Spoel et al., 1997)

$$S_i = \frac{C_{Ra}\lambda\eta\rho_s(1 - \theta_t)}{\theta_a} \quad [2d]$$

with C_{Ra} being the ^{226}Ra concentration of the solids, η the emanation coefficient, and other parameters as defined in Table 1.

The one-dimensional reactive transport Eq. [2] has been solved analytically for a homogeneous vadose zone (Van der Spoel et al., 1997). A ^{222}Rn activity of 0 is used for the upper boundary condition at the soil surface (Eq. [3a]), and a no-flux boundary condition is implemented at the groundwater table at depth L (Eq. [3b]):

$$A = 0 \text{ at } z = 0 \quad [3a]$$

$$\delta A/\delta z = 0 \text{ at } z = L \quad [3b]$$

The solution is then (Van der Spoel et al., 1997)

$$A(z) = \frac{f_i S_i}{\lambda}\left\{1 - \left[\cosh\left(\frac{(L - z)}{\sqrt{\dfrac{f_i D_i}{\lambda}}}\right)\Big/\left[\cosh\left(\frac{L}{\sqrt{\dfrac{f_i D_i}{\lambda}}}\right)\right]\right\} \quad [3c]$$

Note that all parameters with subscript i depend on the characteristics of the vadose zone (i.e., the volumetric water and the NAPL content). These parameters will vary in layered profiles having different characteristics, as listed in Table 2 for various NAPL contents. For media extending to infinite depth, Nazaroff (1992) and Schubert (2001) have given the corresponding analytical model for steady-state profiles in a homogeneous system. The term $f_i S_i/\lambda$ is the asymptote at infinite depth, whereas

Table 1. Parameters and notations used in this study, and values of parameters used for the base case model, given for $T = 20°C$.

Parameter	Notation	Value	Unit	Reference
Production rate of ^{222}Rn in pore space	S_i	1.14×10^{-5}	kBq m^{-3} s^{-1}	obtained from Batch Exp. and Eq. 4
Molecular diffusion coefficient in air	D_m	1.1×10^{-5}	m^2 s^{-1}	Van der Spoel et al. (1997)
Henry's Law constant	H	4.4	–	Wilhelm et al. (1977)
Air–NAPL partitioning coefficient	K_n	0.085 (±0.009)	–	Schubert et al. (2001)
Solid–water partitioning coefficient	K_d	1.4×10^{-5}	m^3 kg^{-1}	Nazaroff (1992)
Decay constant	λ	2.1×10^{-6}	s^{-1}	Nazaroff (1992)
Total porosity	θ_t	0.42	m^3 m^{-3}	†
Volumetric water content	θ_w	0.10	m^3 water m^{-3}	†
Volumetric NAPL content	θ_n	0	m^3 NAPL m^{-3}	
Volumetric air content	θ_a	0.32	m^3 air m^{-3}	
Density of solid phase	ρ_s	2550	kg m^{-3}	†
Depth to groundwater table	L	2.3	m	†

† Parameters were selected to represent as closely as possible the experimental study by Dakhel et al. (2003).

the term $\sqrt{(f_i D_i/\lambda)}$ is also referred to as the characteristic diffusion length.

For heterogeneous layered profiles, the one-dimensional reactive transport Eq. [2] has been solved analytically by the authors, using the software Maple (Vs. 8, Waterloo Maple Inc., Waterloo, Ontario, Canada). At the interface between two adjacent layers (at L_i), constant flux boundary conditions are used according to Fick's first law:

$$\theta_{a1} D_1 \partial A_1/\partial z = \theta_{a2} D_2 \partial A_2/\partial z \text{ at } z = L_i \qquad [3d]$$

For the interpretation of the batch experiments where no diffusive transport is active, Eq. [2a] becomes

$$A_i = f_i S_i/\lambda \qquad [4]$$

MATERIALS AND METHODS

Batch Experiments

Alluvial sand taken from the Rhone delta in Lake Geneva and sieved <4 mm was used for the batch experiments (see Pasteris et al., 2002; Dakhel et al., 2003; Höhener et al., 2003 for detailed properties of the sand). The sand was moistened to a volumetric water content θ_w of 0.10 ± 0.01 before contaminated with the NAPL. *n*-Dodecane having a purity >99% from ACROS Chemicals (distributed by Chemie Brunschwig, Basel, Switzerland) was used as the model NAPL phase (Werner and Höhener, 2002a). The sand and NAPL were mixed in a closed drum and packed immediately into 2.5-L glass bottles sealed with rubber stoppers. Total porosities of 0.43 ± 0.02 were obtained, as gravimetrically determined. A copper tube (≈3 mm, 1/8 inch) was led from the bottom of the bottle through a stopper, and sealed at its end with a valve. After incubation for 20 d at 20°C, a steel needle (1-mm i.d.) was inserted through the rubber stopper for gas extraction from the top of the bottle. The gas within the bottle was circulated by connecting the inlet of a GilAir-3 personal air sampler (Lauper Instruments, Murten, Switzerland) to the steel needle and the outlet to the copper tube. After circulation for 12 min at 700 mL min^{-1}, a 180-mL Lucas cell (EDA Instruments, Toronto, Canada) was introduced into the circulation loop, and the gas was circulated for an additional 2 min through the Lucas cell. Thereafter, the Lucas cell was immediately inserted into the counter chamber of an RD-200 Rn detector (EDA Instruments) and kept for 5 min in the dark. Radon-222 was subsequently counted for periods of 10 min. Blank values from the same Lucas cell were subtracted, and the results were converted to kilobecquerels per cubic meter using a previously established calibration (Surbeck, 1993). Results were adjusted to account for dilution of the soil gas with air initially in the circulation loop and the Lucas cell. The sampling was repeated after an additional incubation of 12 or 15 d.

Lysimeter

Vertical profiles of ^{222}Rn activity were measured in an outdoor lysimeter operated as part of an independent study of the impact of gasoline additives on groundwater quality (Dakhel et al., 2003). The dimensions of the lysimeter were 1.2 m (diameter) by 2.5 m (depth). The porous medium for the unsaturated zone in this lysimeter was the same alluvial sand as used in the batch experiments, packed to a porosity of 0.42. Below the 2.3-m depth, limestone gravel was holding a total of 50 L of groundwater. A siphon at 2.33 m regulated the height of the groundwater table. The height of the capillary fringe in the sand as measured in a laboratory column was 0.07 m (Pasteris et al., 2002). Details of the instrumentation involving gas and water sampling tubes, thermometers and time domain reflectometry (TDR) probes are given elsewhere (Dakhel et al., 2003). On 15 Jan. 2002 (Day 0), sand was excavated to a depth of 1.2 m. A volume of 226 L of this excavated sand was combined with 3.2 L of an artificial gasoline mixture and mixed in a concrete mixer (Dakhel et al., 2003). The contaminated sand was placed between the 1.2- and 1.0-m depths in the lysimeter, and immediately covered with clean sand that was previously excavated. Five soil samples were taken to measure the volumetric NAPL content. The lysimeter was next filled to the top with clean sand within 1.5 h. Volumetric water contents were initially obtained from gravimetric analyses and later from TDR readings each day when VOCs were analyzed in the soil gas, as reported previously in the supporting information section of Dakhel et al. (2003). Vertical profiles of ^{222}Rn in the soil gas were measured on Days 10, 28, and 287 after the artificial contamination with gasoline. With a manual peristaltic

Table 2. Expected variation of the fraction of ^{222}Rn in soil air, f_i, the effective diffusion coefficient, D_i, the characteristic diffusion length $(f_i D_i/\lambda)^{1/2}$ and the production rate of ^{222}Rn in pore space, S_i, as a function of NAPL content, θ_n, for a sandy soil; other parameters are as in Table 1.

Parameter	$\theta_n = 0$ (base case)	$\theta_n = 0.005$	$\theta_n = 0.01$	$\theta_n = 0.02$	$\theta_n = 0.04$	$\theta_n = 0.08$
f_i	0.92	0.79	0.69	0.54	0.37	0.20
D_i, 10^{-6} m^2 s^{-1}	4.38	4.22	4.07	3.77	3.21	2.24
$\sqrt{(f_i D_i/\lambda)}$, m	1.39	1.26	1.16	0.98	0.75	0.46
S_i, 10^{-5} kBq m^{-3} s^{-1}	1.14	1.16	1.18	1.20	1.31	1.52

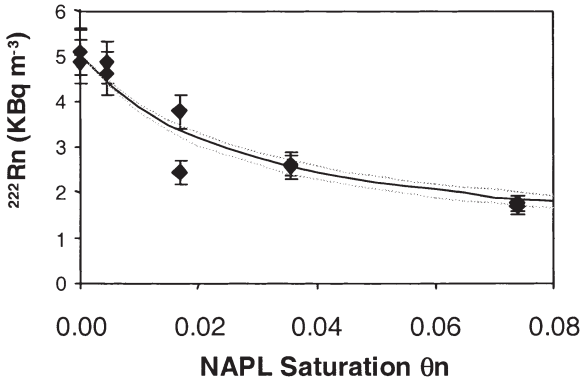

Fig. 1. Measured ^{222}Rn activities in the batch experiments as a function of volumetric NAPL content θ_n (black diamonds, two to three repeated measurements, counting errors of 10%), and predicted ^{222}Rn activities (solid line), using Eq. [4]. Broken lines represent errors of 10% in the air–NAPL partitioning coefficient.

pump connected to the preinstalled soil gas probes (Pasteris et al., 2002), 0.6 L of soil gas were sampled through the Lucas cells and measured immediately on site using procedures as described for the batch experiments.

Measurement of NAPL Content

Soil samples were obtained from the lysimeter using a motor-driven hollow-stem auger of 8-cm diameter (Max Hug, Luzern, Switzerland). The soil was brought to the surface in 0.25-m-long sections. Using a metallic spoon, about 10 g of contaminated soil from samples taken every 5 cm were immediately transferred into vials prefilled with 20 mL of CH_2Cl_2 as extractant. After shaking overnight on a rotary shaker, the extracts were analyzed using gas chromatography as described by (Dakhel et al., 2003). Samples from the batch experiments were analyzed similarly.

RESULTS

Batch Experiments

Figure 1 shows measured ^{222}Rn activities from the batch experiments. In uncontaminated sand at a water content θ_w of 0.1 ± 0.01, a steady-state ^{222}Rn activity of 5.1 ± 0.6 kBq m^{-3} was measured as an average of two batches, each with two replicates. Increasing the volumetric NAPL content caused the steady-state ^{222}Rn activity to decrease; the lowest activity of 1.8 ± 0.2 kBq m^{-3} was found at the highest NAPL content studied (θ_n = 0.074). Except for one sample at θ_n = 0.017, the reproducibility of samples from consecutive incubations was within the counting error. Steady-state ^{222}Rn activities were calculated for different NAPL contents with Eq. [4] (Fig. 1), using S_i values estimated from the uncontaminated batch experiments (Table 1). The measured steady-state activities closely matched the predicted values (Fig. 1).

Analytical Model for Homogeneous Profile

The influence of variable volumetric NAPL content on the ^{222}Rn profile in soil gas was modeled for the homogeneous vadose zone using Eq. [1] and [3c]. The configuration of the model (i.e., depth to groundwater) and the selected parameters for the porous medium (Table 1)

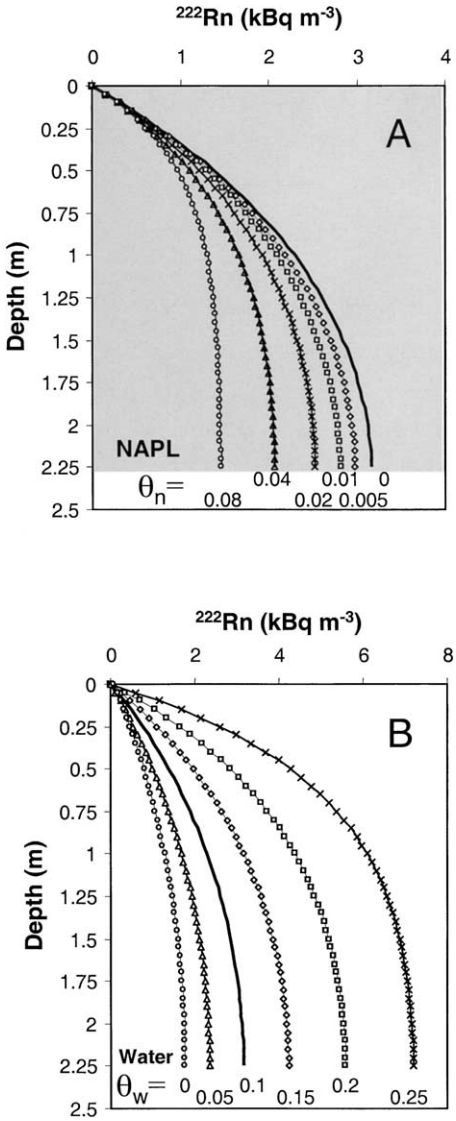

Fig. 2. Modeled ^{222}Rn activities in a homogeneous sandy vadose zone: (A) influence of volumetric NAPL content θ_n and (B) influence of volumetric water content θ_w.

were made as consistent as possible to the lysimeter experiment. Results are shown in Fig. 2A. The predicted ^{222}Rn activities in the uncontaminated vadose zone (base case) increase from 0 to 3.16 kB m^{-3}. Homogeneous contamination of the vadose zone with NAPL caused a decreases in ^{222}Rn activities relative to the base case for every NAPL content. A minimum relative activity of 46% relative to the base case was found immediately above the groundwater table for the highest modeled NAPL content θ_n of 0.08. This is 184 L of NAPL per square meter of vadose zone for a soil column of 2.3-m depth, and corresponds to about 20% NAPL in the pore space. In the case of variable volumetric water contents (Fig. 2B), maximum ^{222}Rn activities are also always observed above the groundwater surface. They increase 2.2-fold when the water contents increase from 0.1 (base case) to 0.25. For a completely dry homogeneous profile, ^{222}Rn activities decreased to 56% of those of the base case (Fig. 2B).

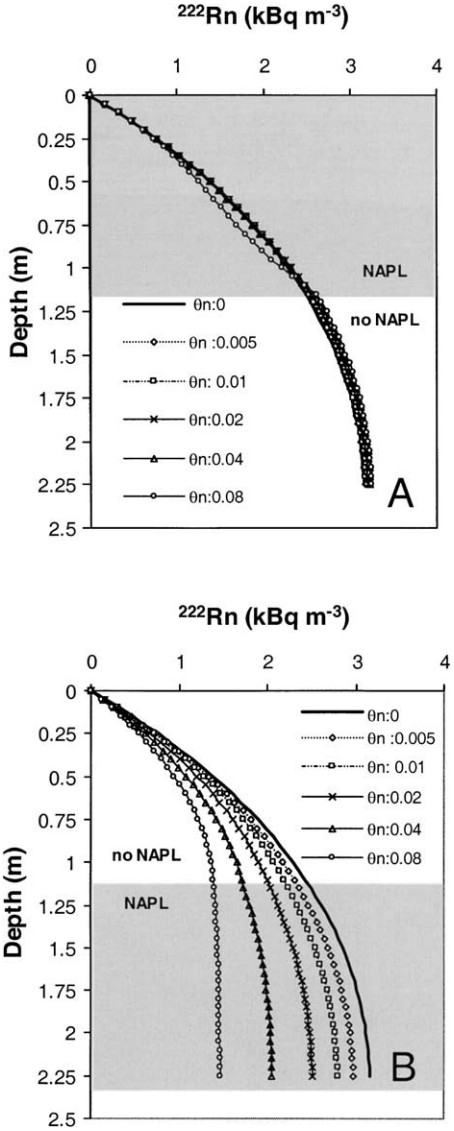

Fig. 3. Modeled ^{222}Rn activities in a heterogeneous sandy vadose zone with two layers of equal thickness having different volumetric NAPL contents θ_n: (A) NAPL contamination in upper layer and (B) NAPL contamination in lower layer.

Analytical Model for Two-Layered Profiles

The influence of variable NAPL content in a two-layered vadose zone was modeled using the analytical solutions given in the Appendix, Part A. Apart from the heterogeneity, the model parameters remained the same as for the homogeneous case. Residual NAPL was placed in an unsealed upper layer of 1.15-m depth, with the lower vadose zone layer assumed to be free of NAPL (Fig. 3A). The total amount of NAPL for the most polluted case was 92 L m^{-2}. The resulting ^{222}Rn depth profiles of the NAPL-contaminated scenarios deviated only slightly from the uncontaminated case (Fig. 3A). A 3% increase in ^{222}Rn activities below the 1.2-m depth was calculated for the situations where the upper layer is contaminated with $\theta_n = 0.08$. The reverse situations (Fig. 3) involved varying NAPL contents in the lower half of the profile. These situations lead to lower ^{222}Rn activities with increased NAPL content, especially in the lower part of the profile. Maximum ^{222}Rn activities for the case when $\theta_n = 0.08$ are 46% of the activities of the base case, similarly as for the homogeneous model.

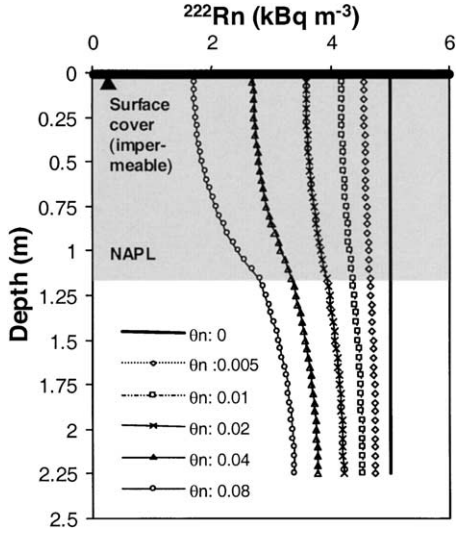

Fig. 4. Modeled ^{222}Rn activities in a heterogeneous sandy vadose zone with a impermeable surface cover. The upper layer is contaminated with NAPL, similarly as in Fig. 3A.

The influence of an impermeable soil cover layer is investigated in Fig. 4, where variable NAPL contents are assumed in the upper profile layer. Constant ^{222}Rn activities of 5 kBq m^{-3} were found at all depths for the uncontaminated case. For the contaminated cases, ^{222}Rn activities decreased with respect to the uncontaminated case. The minimum activity was 1.8 kBq m^{-3} for $\theta_n = 0.08$, directly below the soil cover.

Analytical Model for Three-Layered Profiles

We now show results for an uncovered layered vadose zone with three different layers, of which the intermediate layer is contaminated with NAPL. Results were obtained using the analytical model given in the Appendix, Part B. The configuration is the same the lysimeter experiment. An increasing NAPL content of a layer from the 1- to 1.2-m depth was found to affect the ^{222}Rn profiles as shown in Fig. 5A. The highest NAPL spill corresponded to 16 L m^{-2}. We found that ^{222}Rn activities decreased by up to 20% within and above the contaminated layer. Radon activity distribution below the NAPL layer was not influenced significantly by the NAPL. When a 2-m-deep contaminated layer with $\theta_n = 0.08$ (16 L of NAPL m^{-2}) was placed at different depths in the soil column (Fig. 5B), the ^{222}Rn activities either increased or decreased relative to the base case. For a NAPL residing high in the vadose zone, increases in ^{222}Rn activities will occur below the NAPL layer. For a NAPL residing near the groundwater table at the 2.3-m depth, slight lower ^{222}Rn activities will result throughout the profile (Fig. 5B).

Lysimeter Experiment

Radon-222 activities in the lysimeter were measured 10 and 28 d after contamination with NAPL to allow the

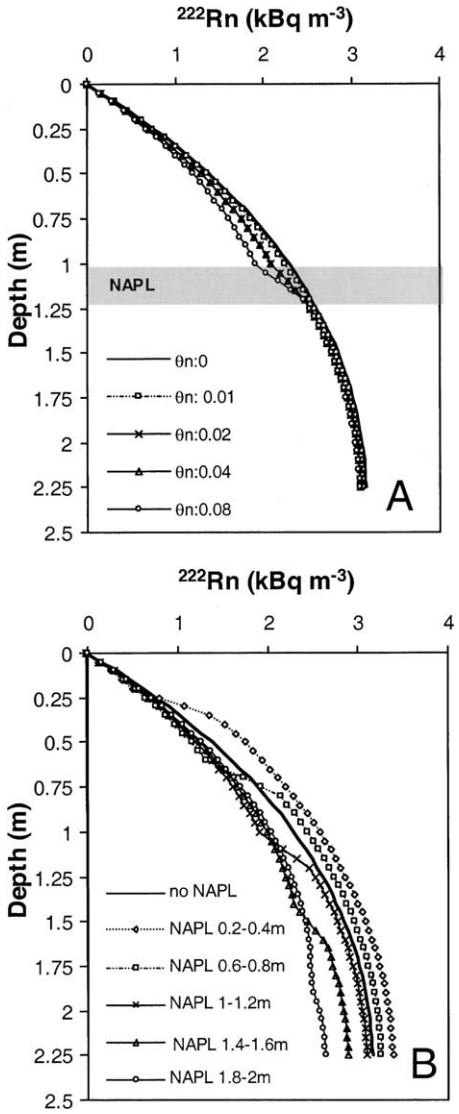

Fig. 5. Modeled ^{222}Rn activities in a heterogeneous sandy vadose zone with three vadose zone layers. (A) Only an intermediate layer from the 1- to 1.2-m depth is contaminated with different volumetric NAPL contents θ_n (corresponding to Fig. 6). (B) A 0.2-m-thick intermediate layer with $\theta_n = 0.08$ (16 L NAPL m^{-2}) is placed at different depths, with L_1 being the depth to contamination.

establishment of steady-state vertical activity profiles. Both profiles showed a steady increase in ^{222}Rn from the soil surface to the 1.1-m depth, followed by a slight decrease to the 1.3-m depth, and then again an increase. Maximum activities of 3.1 and 3.0 kBq m^{-3} were found each day at the 1.7-m depth. The deepest soil gas probe at the 2.1-m depth revealed lower ^{222}Rn activities, particularly on Day 28 (Fig. 6). The ^{222}Rn profile measured on Day 287 showed an increase throughout the lysimeter, with a maximum of 2.9 kBq m^{-3} at the 2.1-m depth. From soil core analyses a NAPL content of 0.01 ± 0.002 (=2 L m^{-2}) was measured at Day 0 between the 1- and 1.2-m depths. The measured NAPL content was slightly lower than the planned content (3.2 L m^{-2}) because of some losses of volatile compounds during packing of the lysimeter. On Day 30, a NAPL content of 0.003 ± 0.002 was found in samples from the 1- to 1.23-m depth,

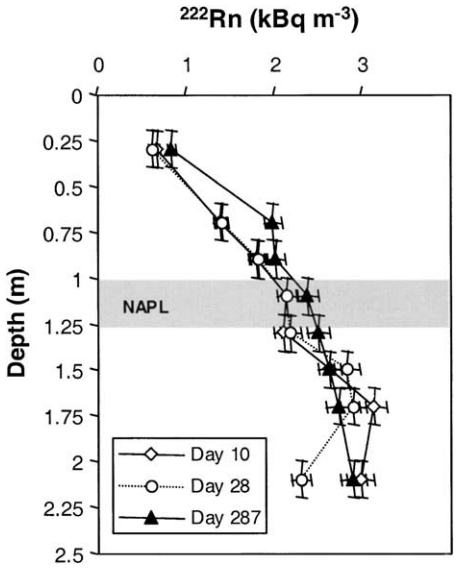

Fig. 6. Measured ^{222}Rn activities in lysimeter experiment. NAPL content θ_n were 0.01 (Day 10), 0.003 (Day 28), and <0.001 on Day 287 in the intermediate layer between 1 and 1.2 m depth. Error bars represent 5% for the activity measurements, and ±0.1 m for depth (accounting for the reach of sampling tubes).

and on Day 287, the NAPL was below the detection limit of 0.001 (Dakhel et al., 2003).

DISCUSSION

Batch Experiments

A nonlinear relationship between ^{222}Rn activity at equilibrium steady-state and NAPL content was found using the batch experiments (Fig. 1). Radon-222 activities decreased by a factor of 2.9 within the range of volumetric NAPL contents typically found in porous media (Mercer and Cohen, 1990). The analytical model (Eq. [1]) predicted the nonlinear decrease quite satisfactorily. Nonlinearity is generated by the interdependency of NAPL and air content (θ_n and θ_a in Eq. [1] and in Eq. [2d]). Assuming overall errors in ^{222}Rn activity measurements of 10%, the smallest NAPL content that can significantly be deduced from batch experiments is $\theta_n = 0.0075$. The air–NAPL partitioning coefficient K_n was measured for gasoline, kerosene, and diesel fuel by Schubert et al. (2001), who reported an uncertainty of ±10.5%. Results of our batch experiments suggest that the K_n from Schubert et al. (2001) is applicable also to our study. We note that similar air–NAPL partitioning coefficients can also be obtained from the Henry coefficient (Table 1) divided by NAPL–water partitioning coefficients, as found in the literature of ^{222}Rn as a tracer for the saturated zone (Hunkeler et al., 1997; Semprini et al., 2000).

Assumptions and Verification of the Transport Model

For this study, we used an existing analytical one-dimensional reactive transport model that was previously verified for homogeneous noncontaminated dry sand column (Van der Spoel et al., 1997) and extended

the model to profiles containing homogeneously and heterogeneously distributed NAPLs. Except for having different fluids, the relevant assumptions of our model are thus the same as used previously (Van der Spoel et al., 1997). The influence of water and NAPL on the diffusion coefficient was modeled by using the classical relationship (Eq. [2c]) developed by Millington and Quirk (1961). Diffusive gas tracer tests in the lysimeter (Werner and Höhener, 2003) previously showed that this relationship gives good estimates for the effective diffusion coefficient. Schubert and Schulz (2002) and Bunzl et al. (1998) investigated processes that were neglected in the model such as gas advection due to atmospheric pressure variations or temperature changes at the soil surface. They found that these processes had only minor impact on steady-state ^{222}Rn profiles. The lower boundary condition used for the model was a no flux condition, thus reflecting a groundwater surface without ^{222}Rn loss. This assumption is sound for stable groundwater tables where the diffusion in the water phase limits the transfer of dissolved ^{222}Rn to soil air. In the case of a retreating water table, a rapid net flux of ^{222}Rn from groundwater to the vadose zone may occur (Cecil and Green, 1999), as experimentally shown for volatile halogenated pollutants in a laboratory column (Werner and Höhener, 2002b). We note in addition that usually a capillary fringe is found above the groundwater table, which may extend significantly into the vadose zone. Models using constant θ_w are expected to produce erroneous results within the capillary fringe. In our lysimeter study, the capillary fringe was, however, limited to <7 cm (Dakhel et al., 2003). The homogeneous model (base case) predicted maximum ^{222}Rn activities of 3.16 kB m^{-3} for the uncontaminated lysimeter using the parameters in Table 1. This agrees with measured activities in the lysimeter (Fig. 6), but is lower than ^{222}Rn activities measured with the uncontaminated batch experiments. The lower activities in the lysimeter can be explained by the lack of a soil cover and diffusive transport of ^{222}Rn to the atmosphere.

Homogeneous Vadose Zone

For a homogeneous vadose zone with unsealed surface, the model predicted that ^{222}Rn activities will vary within a factor of 2.2 for NAPL contents between 0 and 0.08 (Fig. 2A), and within about a factor of 4 for different volumetric water contents between 0 to 0.25 (Fig. 2B). Nonaqueous phase liquids can take up significant amounts of ^{222}Rn, with the fraction in soil air f_i (Eq. [1]) decreasing from 0.92 (noncontaminated) to 0.2 (at θ_n = 0.08, Table 2). Nonaqueous phase liquid also decreases the effective diffusion coefficient by a factor of 2.6 (Table 2). As a result, the characteristic diffusion length of ^{222}Rn in a NAPL-contaminated soil decreases from 1.39 to 0.46 m (Table 2), leading to distributions that approach the large-depth asymptote more quickly than in an uncontaminated profile.

Water increases ^{222}Rn activities in soil air since it occupies pore space that otherwise would be filled with soil air and does not solubilize much ^{222}Rn. A further effect of adding either water or NAPL to a vadose zone is that the production rate of ^{222}Rn in pore space S_i increases as θ_a decreases (Eq. [2d]). The increase was found to be 33% for a NAPL or water content increase of 0.08 (Table 2).

Heterogeneous NAPL Distribution

For the two-layered system with NAPL pollution in the upper half of the profile, local ^{222}Rn minima were found to be indicative for NAPL only for cases where the site is sealed with a soil cover. The model suggests that at sites without an impermeable soil cover, ^{222}Rn measurements will yield relatively little information about the degree of NAPL contamination (Fig. 3A). However, for sites with impermeable soil surface layers, large deviations were found below the surface (Fig. 4). Radon sampling at such sites should then be as shallow as possible.

When the NAPL is in the lower half of the soil profile (e.g., at sites contaminated with lighter-than-water NAPLs floating on groundwater and being dispersed by water table fluctuations in the vadose zone), ^{222}Rn minima will occur in the deeper part of the profile (Fig. 3B). When the NAPL contamination occurs in intermediate vadose zone layers (e.g., due to leaking underground pipelines), the model results (Fig. 5) show that the vertical position, extension, and quantity of NAPL will determine the shape of the ^{222}Rn profile. Radon-222 activities may then increase or decrease. A NAPL-polluted layer relatively high in the vadose zone will lead to an increase in ^{222}Rn in the lower layers with respect to the base case, since the NAPL layer hinders ^{222}Rn diffusion to the atmosphere. Nonaqueous phase liquid layers with thicknesses smaller than the characteristic diffusion length of ^{222}Rn (Table 2) will not markedly influence the ^{222}Rn distributions vs. depth. Given that the characteristic diffusion length at a NAPL content of 0.08 is 0.46 m, it follows that only NAPL layers of this extent or larger will significantly influence the ^{222}Rn profile.

Lysimeter Experiment

The vertical ^{222}Rn profiles obtained in the lysimeter experiment reflect additional difficulties that may be encountered when using ^{222}Rn as a NAPL tracer. First, ^{222}Rn measurements are affected by errors due to sampling and analytical precision, as depicted by the error bars in Fig. 6. The sampling may be biased by the fact that soil gas is drawn from a sphere around a soil gas port. In our case, this sphere had an estimated radius of about 10 cm. The analytical precision is a function of statistics of counting radioactive decay. In this study, sand with a low ^{222}Rn activity was chosen, with counting errors are as high as 10%. As a result of both spatial and analytical errors, ^{222}Rn soil gas profiles measured on Days 10 and 28 when NAPL was present were not statistically different from the profile measured on Day 287 when no NAPL was present, although one measured point at a depth of 1.3 m deviated from the rest. In view of this single point, however, one may not draw conclusions on the presence or absence of NAPL in the profile. We notice here that the experiment involved only a rela-

tively low NAPL content because of the different aims of the original study. The modeled ^{222}Rn profile for θ_n = 0.01 in Fig. 5A suggests that the expected deviation from the base case will be very small. Thus, the experimental data and the modeling results remain within errors of both approaches. Schubert and coworkers injected 25 L of diesel fuel at the 1.2-m depth into a 2-m-deep lysimeter having 1-m^2 surface area (Meissner et al., 2000; Schubert, 2001). They found a decrease in ^{222}Rn activities of more than 50% in the lower part of the lysimeter, and a decrease of about 10% in the upper vadose zone. These findings agree qualitatively with the modeling results in Fig. 3B. However, the exact location of the NAPL at the time of measurement was not reported, and quantification of ^{222}Rn activities in the deeper part of the profile may have been biased by interactions of the diesel fuel with the emplaced in situ Rn probes (Schubert, 2001). The experiment of Schubert and colleagues, however, illustrate that ^{222}Rn activities can be an important indicator of large NAPL spills in the lower half of an artificially constructed vadose zone.

CONCLUSIONS AND OUTLOOK

The batch experiments presented in this study suggest that the naturally occurring noble gas ^{222}Rn is a potential tracer for vadose zone contamination by NAPLs. Sampling and analysis is relatively simple, fast, and easily combined with traditional soil gas monitoring. However, our modeling shows that changes in the equilibrium ^{222}Rn activities due to NAPL contamination are generally less distinct in the field than in batch experiments since diffusive transport of ^{222}Rn has a tendency to smooth the activity gradients, especially when no soil cover is present. For those sites, we do not have a straightforward diagnostic test to positively identify NAPLs at any depth. For sites with impermeable soil covers, ^{222}Rn minima due to NAPL contamination will be much larger. A diagnostic test for NAPL would then involve taking ^{222}Rn samples at shallow depths and compare them with samples from a covered but uncontaminated control location. At real sites, it would be expected that differences in ^{222}Rn activities would also occur due to changes in geology (i.e., changes in Rd concentration, Rn emanation coefficients and porosity). A thorough knowledge of spatial geology changes and analyses of ^{222}Rn profiles in uncontaminated and contaminated locations of the same field site would then be necessary to effectively use ^{222}Rn as a NAPL tracer in vadose zones. Future work should also include possible effects of real problems having a three-dimensional geometry, since the model presented in this study is applicable only to one-dimensional problems.

APPENDIX: ANALYTICAL MODEL FOR LAYERED VADOSE ZONES

Part A: Two Layers

This model describes the scenario with two vadose zone layers of which one is contaminated with NAPL, the other is not. The upper vadose zone extends from $z = 0$ to $z = L_1$, and the lower layer from $z = L_1$ to $z = L$ (total depth). Nonaqueous phase liquid influences all parameters with subscript i (see Tables 1 and 2 of manuscript for notations and values). At the soil surface $z = 0$, the ^{222}Rn concentration is zero. At $z = L$, there is a groundwater table with a zero flux boundary condition. First, we calculate the profile in the upper vadose zone ($0 < z < L_1$) and set the unknown gradient at the layer boundary as x. We calculate the Rn activity profile governed by diffusion, decay, and production at steady state. The governing equation and boundary conditions for the upper profile are

$$f_1 D_1\left[\frac{d^2}{dz^2}A(z)\right] - \lambda A(z) + f_1 S_1 = 0 \qquad A(0) = 0$$

$$D(A)(L_1)\theta_1 D_1 = x$$

The analytical solution for depth $0 < z < L_1$ was found by using the software Maple (Vs. 8, Waterloo Maple Inc.):

$$A(z) = -\frac{e\left(\frac{\sqrt{\lambda}\, z}{\sqrt{f_1}\sqrt{D_1}}\right)\left[\theta_1 D_1 f_1 S_1 - x\sqrt{f_1}\sqrt{D_1}\, e\left(\frac{\sqrt{\lambda}\, L_1}{\sqrt{f_1}\sqrt{D_1}}\right)\sqrt{\lambda}\right]}{\theta_1 D_1 \lambda\left\{\left[e\left(\frac{\sqrt{\lambda}\, L_1}{\sqrt{f_1}\sqrt{D_1}}\right)\right]^2 + 1\right\}} -$$

$$\frac{e\left(\frac{-\sqrt{\lambda}\, z}{\sqrt{f_1}\sqrt{D_1}}\right) e\left(\frac{\sqrt{\lambda}\, L_1}{\sqrt{f_1}\sqrt{D_1}}\right)\left[x\sqrt{f_1}\sqrt{D_1}\sqrt{\lambda} + \theta_1 D_1 f_1 S_1 e\left(\frac{\sqrt{\lambda}\, L_1}{\sqrt{f_1}\sqrt{D_1}}\right)\right]}{\theta_1 D_1 \lambda\left\{\left[e\left(\frac{\sqrt{\lambda}\, L_1}{\sqrt{f_1}\sqrt{D_1}}\right)\right]^2 + 1\right\}} + \frac{f_1 S_1}{\lambda}$$

For the profile in the lower vadose zone, the equations are

$$f_2 D_2\left[\frac{d^2}{dz^2}A(z)\right] - \lambda A(z) + f_2 S_2 = 0$$

$$D(A)(L_1)\,\theta_2 D_2 = x \qquad D(A)(L) = 0$$

The analytical solution valid for depths $L_1 < z < L$ is

$$A(z) = -\frac{e\left(\frac{\sqrt{\lambda}\, z}{\sqrt{f_2}\sqrt{D_2}}\right) x\sqrt{f_2}\, e\left(\frac{\sqrt{\lambda}\, L_1}{\sqrt{f_2}\sqrt{D_2}}\right)}{\sqrt{D_2}\sqrt{\lambda}\,\theta_2\left\{-\left[e\left(\frac{\sqrt{\lambda}\, L_1}{\sqrt{f_2}\sqrt{D_2}}\right)\right]^2 + \left[e\left(\frac{\sqrt{\lambda}\, L}{\sqrt{f_2}\sqrt{D_2}}\right)\right]^2\right\}} -$$

$$\frac{e\left(-\frac{\sqrt{\lambda}\, z}{\sqrt{f_2}\sqrt{D_2}}\right) x\sqrt{f_2}\, e\left(\frac{\sqrt{\lambda}\, L_1}{\sqrt{f_2}\sqrt{D_2}} + \frac{2\sqrt{\lambda}\, L}{\sqrt{f_2}\sqrt{D_2}}\right)}{\sqrt{D_2}\sqrt{\lambda}\,\theta_2\left\{-\left[e\left(\frac{\sqrt{\lambda}\, L_1}{\sqrt{f_2}\sqrt{D_2}}\right)\right]^2 + \left[e\left(\frac{\sqrt{\lambda}\, L}{\sqrt{f_2}\sqrt{D_2}}\right)\right]^2\right\}} + \frac{f_2 S_2}{\lambda}$$

The boundary condition at L_1 is given in the manuscript (Eq. [3d]). The unknown activity gradient x at the boundary at L_1 is found by setting $A(z = L_1)$ of the upper profile = $A(z = L_1)$ of the lower profile and solving for x. This gave:

$$\left(x = \sqrt{D_2}\,\theta_2\,\theta_1 D_1\left[2\, e\left(\frac{\sqrt{\lambda}\, L_1(\sqrt{f_2}\sqrt{D_2} + 2\sqrt{f_1}\sqrt{D_1})}{\sqrt{f_1}\sqrt{D_1}\sqrt{f_2}\sqrt{D_2}}\right) f_1 S_1 -\right.$$

$$2\, e\left(\frac{\sqrt{\lambda}\,(L_1\sqrt{f_2}\sqrt{D_2} + 2L\sqrt{f_1}\sqrt{D_1})}{\sqrt{f_1}\sqrt{D_1}\sqrt{f_2}\sqrt{D_2}}\right) f_1 S_1 -$$

$$f_2 S_2\, e\left(\frac{2\sqrt{\lambda}\,(L_1\sqrt{f_2}\sqrt{D_2} + L\sqrt{f_1}\sqrt{D_1})}{\sqrt{f_1}\sqrt{D_1}\sqrt{f_2}\sqrt{D_2}}\right) +$$

$$f_2 S_2\, e\left(\frac{2\sqrt{\lambda}\, L_1}{\sqrt{f_2}\sqrt{D_2}}\right) - f_2 S_2\, e\left(\frac{2\sqrt{\lambda}\, L}{\sqrt{f_2}\sqrt{D_2}}\right) + f_1 S_1\, e\left(\frac{2\sqrt{\lambda}\, L}{\sqrt{f_2}\sqrt{D_2}}\right) -$$

$$f_1 S_1\, e\left(\frac{2\sqrt{\lambda}\, L_1(\sqrt{f_2}\sqrt{D_2} + \sqrt{f_1}\sqrt{D_1})}{\sqrt{f_1}\sqrt{D_1}\sqrt{f_2}\sqrt{D_2}}\right) +$$

$$f_1 S_1 \mathrm{e}\left(\frac{2\sqrt{\lambda}\,(L_1\sqrt{f_2}\sqrt{D_2} + L\sqrt{f_1}\sqrt{D_1})}{\sqrt{f_1}\sqrt{D_1}\sqrt{f_2}\sqrt{D_2}}\right) -$$

$$f_1 S_1 \mathrm{e}\left(\frac{2\sqrt{\lambda}\,L_1}{\sqrt{f_2}\sqrt{D_2}}\right) + f_2 S_2 \mathrm{e}\left(\frac{2\sqrt{\lambda}\,L_1\,(\sqrt{f_2}\sqrt{D_2} + \sqrt{f_1}\sqrt{D_1})}{\sqrt{f_1}\sqrt{D_1}\sqrt{f_2}\sqrt{D_2}}\right)\Bigg] \Bigg/$$

$$\Bigg\{\sqrt{\lambda}\Bigg[\mathrm{e}\left(\frac{2\sqrt{\lambda}\,L_1\,(\sqrt{f_2}\sqrt{D_2} + \sqrt{f_1}\sqrt{D_1})}{\sqrt{f_1}\sqrt{D_1}\sqrt{f_2}\sqrt{D_2}}\right)\sqrt{D_2}\,\theta_2\sqrt{f_1}\sqrt{D_1} -$$

$$\mathrm{e}\left(\frac{2\sqrt{\lambda}\,(L_1\sqrt{f_2}\sqrt{D_2} + L\sqrt{f_1}\sqrt{D_1})}{\sqrt{f_1}\sqrt{D_1}\sqrt{f_2}\sqrt{D_2}}\right)\sqrt{D_2}\,\theta_2\sqrt{f_1}\sqrt{D_1} -$$

$$\mathrm{e}\left(\frac{2\sqrt{\lambda}\,L_1}{\sqrt{f_2}\sqrt{D_2}}\right)\sqrt{D_2}\,\theta_2\sqrt{f_1}\sqrt{D_1} + \mathrm{e}\left(\frac{2\sqrt{\lambda}\,L}{\sqrt{f_2}\sqrt{D_2}}\right)\sqrt{D_2}\,\theta_2\sqrt{f_1}\sqrt{D_1} -$$

$$\mathrm{e}\left(\frac{2\sqrt{\lambda}\,L_1\,(\sqrt{f_2}\sqrt{D_2} + \sqrt{f_1}\sqrt{D_1})}{\sqrt{f_1}\sqrt{D_1}\sqrt{f_2}\sqrt{D_2}}\right)\sqrt{f_2}\,\theta_1 D_1 - \mathrm{e}\left(\frac{2\sqrt{\lambda}\,L_1}{\sqrt{f_2}\sqrt{D_2}}\right)\sqrt{f_2}\,\theta_1 D_1 -$$

$$\mathrm{e}\left(\frac{2\sqrt{\lambda}\,(L_1\sqrt{f_2}\sqrt{D_2} + L\sqrt{f_1}\sqrt{D_1})}{\sqrt{f_1}\sqrt{D_1}\sqrt{f_2}\sqrt{D_2}}\right)\sqrt{f_2}\,\theta_1 D_1 -$$

$$\mathrm{e}\left(\frac{2\sqrt{\lambda}\,L}{\sqrt{f_2}\sqrt{D_2}}\right)\sqrt{f_2}\,\theta_1 D_1\Bigg]\Bigg)\Bigg)$$

Part B: Three Vadose Zone Layers

Three vadose zone layers are present in this scenario: the upper layer extends from $z = 0$ to $z = L_1$ and is not contaminated, the intermediate layer extends from $z = L_1$ to $z = L_2$ and contains NAPL, and the lower layer from $z = L_2$ to $z = L$ (total depth) is free of NAPL again. The same equations and boundary conditions as in Part A apply, except that two unknown boundary conditions exist at $z = L_1$ and at $z = L_2$ (see Eq. [3d]). The analytical solutions were found again using the Maple software. They are not printed here for sake of brevity.

ACKNOWLEDGMENTS

This study benefited from cooperation within the European project Groundwater Risk Assessment at Contaminated Sites, GRACOS, EVK1-CT-1999-00029. The authors thank D. Werner, D. Hunkeler, two unknown reviewers, Associate Editor Y. Yortsos, and Editor R. van Genuchten for comments on the model and the manuscript, and G. Pasteris and N. Dakhel for operating the lysimeter.

REFERENCES

Boulding, R.J. 1996. EPA environmental assessment sourcebook. Ann Arbor Press, Chelsea, MI.

Brusseau, M.L., N.T. Nelson, and M.S. Costanza-Robinson. 2003. Partitioning tracer tests for characterizing immiscible-fluid saturations and interfacial areas in the vadose zone. Available at www.vadosezonejournal.org. Vadose Zone J. 2:138–147.

Bunzl, K., F. Ruckerbauer, and R. Winkler. 1998. Temporal and small-scale spatial variability of Rn-222 gas in a soil with a high gravel content. Sci. Total Environ. 220:157–166.

Cecil, L.D., and J.R. Green. 1999. Radon-222. p. 175–195. *In* P. Cook and A. Herczeg (ed.) Environmental tracers in subsurface hydrogeology. Kluwer, Boston.

Dakhel, N., G. Pasteris, D. Werner, and P. Höhener. 2003. Small-volume releases of gasoline in the vadose zone: Impact of the additives MTBE and ethanol on groundwater quality. Environ. Sci. Technol. 37:2127–2133.

Davis, B.M., J.D. Istok, and L. Semprini. 2002. Push-pull partitioning tracer tests using radon-222 to quantify non-aqueous phase liquid contamination. J. Contam. Hydrol. 58:129–146.

Deeds, N.E., G.A. Pope, and D.C. McKinney. 1999. Vadose zone characterization at a contaminated field site using partitioning interwell tracer technology. Environ. Sci. Technol. 33:2745–2751.

Dwarakanath, V., N. Deeds, and G.A. Pope. 1999. Analysis of partitioning interwell tracer tests. Environ. Sci. Technol. 33:3829–3836.

Feenstra, S., and J.A. Cherry. 1996. Diagnosis and assessment of DNAPL sites. p. 395–473. *In* J.F. Pankow and J.A. Cherry (ed.) Dense chlorinated solvents and other DNAPL sites. Waterloo Press, Portland, OR.

Hoehn, E., and H.R. von Gunten. 1989. Radon in groundwater: A tool to assess infiltration from surface waters to aquifers. Water Resour. Res. 25:1795–1803.

Höhener, P., C. Duwig, G. Pasteris, K. Kaufmann, N. Dakhel, and H. Harms. 2003. Biodegradation of petroleum hydrocarbon vapors: Laboratory studies on rates and kinetics in unsaturated alluvial sand. J. Contam. Hydrol. 66:93–115.

Hunkeler, D., E. Hoehn, P. Höhener, and J. Zeyer. 1997. ^{222}Rn as a partitioning tracer to detect mineral oil contaminations: Laboratory experiments and field study. Environ. Sci. Technol. 31:3180–3187.

Looney, B.B., and R.W. Falta. 2000. Vadose zone. Vol. 1. Battelle Press, Columbus, OH.

Mariner, P.E., M.Q. Jin, J.E. Studer, and G.A. Pope. 1999. The first vadose zone partitioning interwell tracer test for nonaqueous phase liquid and water residual. Environ. Sci. Technol. 33:2825–2828.

Meissner, R., H. Rupp, and M. Schubert. 2000. Novel lysimeter techniques—A basis for the improved investigation of water, gas, and solute transport in soils. J. Plant Nutr. Soil Sci. 163:603–608.

Mercer, J.W., and R.M. Cohen. 1990. A review of immiscible fluids in the subsurface: Properties, models, characterization, and remediation. J. Contam. Hydrol. 6:107–126.

Millington, R., and J.P. Quirk. 1961. Permeability of porous solids. Trans. Faraday Soc. 57:1200–1207.

Nazaroff, W.W. 1992. Radon transport from soil to air. Rev. Geophys. 30:137–160.

Pasteris, G., D. Werner, K. Kaufmann, and P. Höhener. 2002. Vapor phase transport and biodegradation of volatile fuel compounds in the unsaturated zone: A large scale lysimeter experiment. Environ. Sci. Technol. 36:30–39.

Robbins, G.A., B.G. Deyo, M.R. Temple, J.D. Stuart, and M.J. Lacy. 1990. Soil-gas surveying for subsurface gasoline contamination using total organic vapor detection instruments. Part I. Theory and laboratory experimentation. Ground Water Monit. Remed. 10: 122–131.

Schubert, M. 2001. Detection of subsurface contamination by NAPLs with the aid of radon measurements in soil air. (In German.) Ph.D. diss. Umweltforschungszentrum Leipzig-Halle, Leipzig-Halle.

Schubert, M., K. Freyer, H.C. Treutler, and H. Weiss. 2000. Radon-222 as an indicator of subsurface NAPL contamination. p. 127–128. *In* P.L. Bjerg et al. (ed.) Groundwater 2000. Balkema, Rotterdam, The Netherlands.

Schubert, M., K. Freyer, H.C. Treutler, and H. Weiss. 2001. Using the soil gas radon as an indicator for ground contamination by non-aqueous phase-liquids. J. Soils Sediments 1:217–222.

Schubert, M., K. Freyer, H.C. Treutler, and H. Weiss. 2002. Using radon-222 in soil gas as an indicator of subsurface contamination by non-aqueous phase-liquids (NAPLs). Geofisica Internacional 41:433–437.

Schubert, M., and H. Schulz. 2002. Diurnal radon variations in the upper soil layers and at the soil–air interface related to meteorological parameters. Health Phys. 83:91–96.

Semprini, L., O.S. Hopkins, and B.R. Tasker. 2000. Laboratory, field and modeling studies of radon-222 as a natural tracer for monitoring NAPL contamination. Transp. Porous Media 38:223–240.

Surbeck, H. 1993. Radon monitoring in soils and water. Nucl. Tracks Radiat. Meas. 22:463–468.

Van der Spoel, W.H., E.R. Van der Graf, and R.J. deMeijer. 1997. Diffusive transport of radon in homogeneous column of dry sand. Health Phys. 72:766–778.

Werner, D. 2002. Gaseous tracer diffusion from a point source as a site investigation method. Ph.D. diss. Swiss Federal Institute of Technology, Lausanne, Switzerland.

Werner, D., M. Broholm, and P. Höhener. 2004. Simultaneous measurement of nonaqueous phase liquid (NAPL) saturation and diffusive fluxes of volatile organic compounds in the vadose zone. Ground Water Monitor. Remed. (in press).

Werner, D., and P. Höhener. 2002a. Diffusive partitioning tracer test for nonaqueous phase liquid (NAPL) detection in the vadose zone. Environ. Sci. Technol. 36:1592–1599.

Werner, D., and P. Höhener. 2002b. The influence of water table fluctuations on the volatilization of contaminants from groundwater. p. 213–218. *In* S.F. Thornton and S.E. Oswald (ed.) Groundwater quality: Natural and enhanced restoration of groundwater pollution. Proceedings of the Groundwater Quality Conference, Sheffield, UK. June 2001. IAHS Publ. 275. IAHS Press, Wallingford, UK.

Werner, D., and P. Höhener. 2003. In situ method to measure effective and sorption-affected gas-phase diffusion coefficients in soils. Environ. Sci. Technol. 37:2502–2510.

Whitley, G.A., D.C. McKinney, G.A. Pope, B.A. Rouse, and N.E. Deeds. 1999. Contaminated vadose zone characterization using partitioning gas tracers. J. Environ. Eng. 125:574–582.

Wiedemeier, T.H., H.S. Rifai, C.J. Newell, and J.T. Wilson. 1999. Natural attenuation of fuels and chlorinated solvents in the subsurface. John Wiley and Sons, New York.

Wiegand, J. 2001. A guideline for the evaluation of the soil radon potential based on geogenic and anthropogenic parameters. Environ. Geol. 40:949–963.

Wilhelm, E., R. Battino, and R.J. Wilcock. 1977. Low-pressure solubility of gases in liquid water. Chem. Rev. 77:219–262.

Wilson, D.J. 1997. Soil gas volatile organic compound concentration contours for locating vadose zone nonaqueous phase liquid contamination. Environ. Monit. Assess. 48:73–100.